Assessing hemoglobin concentration using spectroscopic optical coherence tomography for feasibility of tissue diagnostics

Francisco E. Robles,[1,2] Shwetadwip Chowdhury,[1] and Adam Wax[1,2,*]

[1]*Department of Biomedical Engineering and Fitzpatrick Institute for Photonics, Duke University, Durham NC 27708, USA*
[2]*Medical Physics Program, Duke University, Durham NC 27708, USA*
**a.wax@duke.edu*

Abstract: Hemoglobin (Hb) concentration and oxygen saturation levels are important biomarkers for various diseases, including cancer. Here, we investigate the ability to measure these parameters for tissue using spectroscopic optical coherence tomography (SOCT). A parallel frequency domain OCT system is used with detection spanning the visible region of the spectrum (450 nm to 700 nm). Oxygenated and deoxygenated Hb absorbing phantoms are analyzed. The results show that Hb concentrations as low as 1.2 g/L at 1 mm can be retrieved indicating that both normal and cancerous tissue measurements may be obtained. However, measurement of oxygen saturation levels may not be achieved with this approach.

OCIS codes: (170.1470) Blood or tissue constituent monitoring; (170.6510) Spectroscopy, tissue diagnostics; (300.1030) Absorption; (110.4500) Optical coherence tomography.

References and links:

1. P. Carmeliet, and R. K. Jain, "Angiogenesis in cancer and other diseases," Nature **407**(6801), 249–257 (2000).
2. A. Dhar, K. S. Johnson, M. R. Novelli, S. G. Bown, I. J. Bigio, L. B. Lovat, and S. L. Bloom, "Elastic scattering spectroscopy for the diagnosis of colonic lesions: initial results of a novel optical biopsy technique," Gastrointest. Endosc. **63**(2), 257–261 (2006).
3. H. W. Wang, J. K. Jiang, C. H. Lin, J. K. Lin, G. J. Huang, and J. S. Yu, "Diffuse reflectance spectroscopy detects increased hemoglobin concentration and decreased oxygenation during colon carcinogenesis from normal to malignant tumors," Opt. Express **17**(4), 2805–2817 (2009).
4. A. Amelink, H. J. Sterenborg, M. P. Bard, S. A. Burgers, and S. Burgers, "In vivo measurement of the local optical properties of tissue by use of differential path-length spectroscopy," Opt. Lett. **29**(10), 1087–1089 (2004).
5. D. Huang, E. A. Swanson, C. P. Lin, J. S. Schuman, W. G. Stinson, W. Chang, M. R. Hee, T. Flotte, K. Gregory, C. A. Puliafito, and J. Fujimoto, "Optical coherence tomography," Science **254**(5035), 1178–1181 (1991).
6. U. Morgner, W. Drexler, F. X. Kärtner, X. D. Li, C. Pitris, E. P. Ippen, and J. G. Fujimoto, "Spectroscopic optical coherence tomography," Opt. Lett. **25**(2), 111–113 (2000).
7. C. Xu, P. Carney, and S. Boppart, "Wavelength-dependent scattering in spectroscopic optical coherence tomography," Opt. Express **13**(14), 5450–5462 (2005).
8. F. E. Robles, and A. Wax, "Measuring morphological features using light-scattering spectroscopy and Fourier-domain low-coherence interferometry," Opt. Lett. **35**(3), 360–362 (2010).
9. D. J. Faber, E. G. Mik, M. C. Aalders, and T. G. van Leeuwen, "Light absorption of (oxy-)hemoglobin assessed by spectroscopic optical coherence tomography," Opt. Lett. **28**(16), 1436–1438 (2003).
10. N. Bosschaart, M. C. Aalders, D. J. Faber, J. J. Weda, M. J. van Gemert, and T. G. van Leeuwen, "Quantitative measurements of absorption spectra in scattering media by low-coherence spectroscopy," Opt. Lett. **34**(23), 3746–3748 (2009).
11. F. Robles, R. N. Graf, and A. Wax, "Dual window method for processing spectroscopic optical coherence tomography signals with simultaneously high spectral and temporal resolution," Opt. Express **17**(8), 6799–6812 (2009).
12. R. N. Graf, F. E. Robles, X. Chen, and A. Wax, "Detecting precancerous lesions in the hamster cheek pouch using spectroscopic white-light optical coherence tomography to assess nuclear morphology via spectral oscillations," J. Biomed. Opt. **14**(6), 064030 (2009).
13. R. N. Graf, W. J. Brown, and A. Wax, "Parallel frequency-domain optical coherence tomography scatter-mode imaging of the hamster cheek pouch using a thermal light source," Opt. Lett. **33**(12), 1285–1287 (2008).

#129416 - $15.00 USD Received 1 Jun 2010; revised 16 Jul 2010; accepted 16 Jul 2010; published 27 Jul 2010

14. K. Dalziel, and J. R. O'Brien, "Side reactions in the deoxygenation of dilute oxyhaemoglobin solutions by sodium dithionite," Biochem. J. **67**(1), 119–124 (1957).
15. S. Prahl, "Optical Absorption of Hemoglobin " (1999), *http://omlc.ogi.edu/spectra/hemoglobin/*.
16. D. J. Faber, E. G. Mik, M. C. Aalders, and T. G. van Leeuwen, "Toward assessment of blood oxygen saturation by spectroscopic optical coherence tomography," Opt. Lett. **30**(9), 1015–1017 (2005).
17. D. J. Faber, and T. G. van Leeuwen, "Are quantitative attenuation measurements of blood by optical coherence tomography feasible?" Opt. Lett. **34**(9), 1435–1437 (2009).
18. C. Xu, D. Marks, M. Do, and S. Boppart, "Separation of absorption and scattering profiles in spectroscopic optical coherence tomography using a least-squares algorithm," Opt. Express **12**(20), 4790–4803 (2004).
19. F. Robles, and A. Wax, "Separating the scattering and absorption coefficients using the real and imaginary parts of the refractive index with low coherence interferometry," Opt. Lett. (in review).

1. Introduction

Multiple disorders affect tissue blood content and oxygen levels, including infectious processes, polyps, and cancer [1]; hence, knowledge of these parameters can be very instrumental in diagnosing diseases. To obtain this information, optical techniques can take advantage of the very distinct absorption features of oxygenated (oxy-) and deoxygenated (deoxy-) hemoglobin (Hb), and have the ability to provide noninvasive, *in-vivo* monitoring. However, current optical techniques for this purpose, including pulse oximetry, elastic light spectroscopy [2], diffuse reflectance spectroscopy [3], and differential path length spectroscopy [4], suffer from poor spatial resolution, thus only obtaining tissue properties averaged over large volumes. These methods are also unable to obtain precise information regarding the trajectories of the measured photons; as a result, parameters of interest, including absorption, are estimated by employing empirical and/or Monte Carlo simulations rather than physical models. These shortcomings have motivated the development of other methods that may improve diagnostic efficacy by providing better spatial information and insight to tissue properties by means of physical models. One such method is spectroscopic optical coherence tomography (SOCT).

Optical coherence tomography (OCT) is an imaging modality based on low-coherence interferometry (LCI) that provides noninvasive, high resolution, cross-sectional images of biological samples [5]. Advances in OCT have allowed for acquisition of depth-resolved functional information using SOCT [6–8], introducing the possibility to improve current clinical methods for quantifying tissue properties *in vivo* [9,10]. Compared to the other optical techniques mentioned above, SOCT provides spectroscopic information with high spatial resolution allowing for functional information to be directly overlaid with images of tissue structure. Additionally, SOCT measures singly scattered light, thereby allowing the use of more simple physical models, such as Beer's law.

To obtain depth resolved spectroscopic information, SOCT typically employs short-time Fourier Transforms (STFT) or continuous wavelet transforms (CWT). Unfortunately, these operations suffer from an inherent trade-off between spatial and spectral resolution that has limited the ability to quantitatively process depth resolved spectra. To ameliorate this trade off, the dual-window (DW) method for processing SOCT signals was developed. The DW method is simply the product of two STFT's with different window sizes, which, if judiciously chosen, can be used to independently tune the spatial and spectral resolution [11]. We have demonstrated the use of the DW for SOCT, in combination with Fourier domain LCI (fLCI) and light scattering spectroscopy (LSS), to probe morphological features in tissue phantoms [8], and for obtaining cell nuclear size to diagnose malignant states in *ex-vivo* tissue samples [12].

In this paper, we demonstrate the ability to quantitatively measure depth resolved absorption spectra to extract a wide range of absorber concentrations using oxy- and deoxy-Hb phantoms. Further, we investigate the lower limit of Hb concentration and percent oxygen saturation that can be obtained using our system to determine the feasibility of characterizing Hb absorption in tissue.

#129416 - $15.00 USD Received 1 Jun 2010; revised 16 Jul 2010; accepted 16 Jul 2010; published 27 Jul 2010

2. Materials and methods

2.1 System design

A parallel frequency domain OCT system (pfdOCT) is used, which consists of a Michelson interferometer geometry for coherence gating, with the addition of 4 lenses that form a 4-F imaging system for parallel detection [13]. A series of spectral filters are used to shape the light emitting from a super continuum light source (Fianium, Eugene, OR) that is then collimated onto the sample and reference mirror using L2 and L3/L4 as illustrated in Fig. 1. Then, using lenses L3/L4 and L5, the scattered and reflected light from the sample and reference mirror, respectively, is imaged on to the entrance slit of an imaging spectrograph (Princeton Instruments, Trenton NJ). This configuration allows simultaneous (or parallel) detection of multiple interferograms.

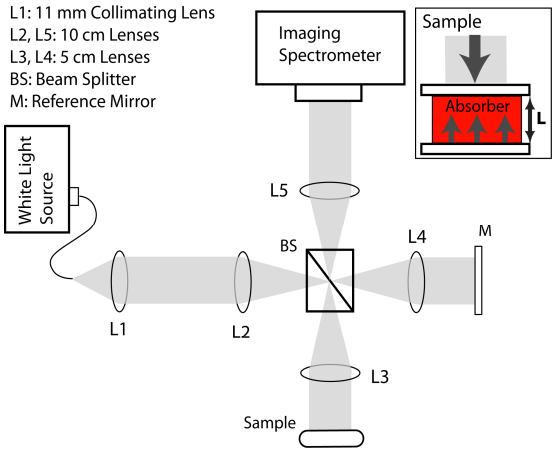

Fig. 1. Parallel frequency domain OCT system and sample. ***L*** ≈400 μm is the thickness of the Hb absorbing phantom.

2.2 Sample preparation and detection

Oxy- and deoxy- Hb samples were prepared at varying concentrations ranging from ~5 g/L to 70 g/L (~78 μM to 1085 μM). For the oxy-Hb samples, human ferrous stable Hb in lyophilized powder form (Sigma-Aldrich, St. Louis, MO) was diluted in purified water until the desired concentration was achieved. To produce deoxy-Hb, a trace amount of sodium dithionite, which removes the oxygen in oxy-Hb, was introduced to a solution of the Hb powder and phosphate buffered saline (PBS). The use of PBS here is to assure that reactions that degrade specific absorption do not occur [14]. The samples were then placed in a container composed of two glass slides separated by spacers of thickness L ≈400 μm, as seen in the inset of Fig. 1.

For detection, the grating in the system's imaging spectrograph is set to operate in the visible region of the spectrum, centered about 575 nm with a bandwidth of ~250 nm. As seen in Fig. 2(a), this spectral range corresponds to a region of significant Hb attenuation, thus leading to higher sensitivity for detecting absorption compared to other OCT systems that operate at near infrared wavelengths [5]. From Fig. 2(b), one can also observe that, in this range, the absorption coefficients of oxy- and deoxy- Hb are significantly different, thereby allowing Hb oxygenation saturation states to be measured. A more thorough discussion is included in section 3.3.

#129416 - $15.00 USD Received 1 Jun 2010; revised 16 Jul 2010; accepted 16 Jul 2010; published 27 Jul 2010

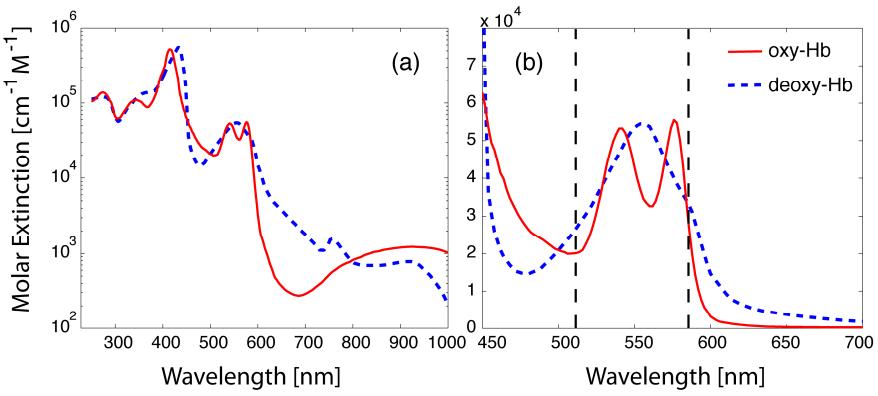

Fig. 2. Molar extinction coefficients of oxy-/deoxy- Hb over a large spectral range (a), and across the visible region of the spectrum (b). The dotted black lines in (b) delineate the region where the oxy- and deoxy- Hb coefficients exhibit the greatest dissimilarity (correlation R~0). Data compiled by Prahl [15].

3. Results

3.1 Absorption profiles

The data were acquired from the Hb samples using the pfdOCT system. The signal from a single lateral channel (A-scan) may de described by,

$$\tilde{I} = I_r + I_s + 2\sqrt{I_s I_r}\cos\left(k \cdot 2\Delta OPL\right), \tag{1}$$

where I_r is the reference field intensity, I_s is the sample field intensity, ΔOPL is the optical path length difference between the sample and reference arms, and k is the wavenumber ($k = 2\pi/\lambda$). The non-interferometric terms in the signal ($I_r + I_s$) were eliminated using subtraction of separate background acquisitions, and the source's spectral dependence was removed by normalizing by the reference field. The resulting interferogram was processed using the DW method with Gaussian window sizes w_1 = 0.061 μm^{-1} and w_2 = 0.907 μm^{-1} to yield depth-resolved spectroscopic information with spatial resolution of 3.05 μm and spectral resolution of 3.20 nm. The experimental spatial resolution of the pfdOCT system is ~1.10 μm.

The spectrum from the front of the rear cover glass of the sample, corresponding to an absorber thickness of 400μm, was recorded (see inset of Fig. 1). Since the light only experiences attenuation, the intensity of the processed depth resolved spectrum is described by Beer's law,

$$I(\lambda, L) = rI_0 \exp\left(-\mu_a(\lambda)L\right). \tag{2}$$

where $\mu_a(\lambda)$ is the wavelength- and concentration-dependent attenuation coefficient, $\boldsymbol{r}$ is the reflectivity (or scattering cross section) of the sample, and L is the physical thickness of the absorber. The initial light intensity, I_0, is measured from the same surface in absence of oxy-/deoxy- Hb, using water or PBS as the sample. Furthermore, note that the intensity depends on L and not $2L$ resulting from the square root term in Eq. (1). Figures 3(a) and 3(b) illustrate representative experimental normalized oxy- and deoxy- Hb intensity profile, respectively, obtained after processing. The theoretical absorption curves (dotted black lines) are also plotted. Figures 3(c) and 3(d) are the corresponding attenuation coefficients. Note that the ideal and the measured profiles are in excellent agreement, where the absorption peaks at 540 nm and 575 nm for oxy-Hb, and at 555 nm for deoxy-Hb are clearly evident.

#129416 - $15.00 USD Received 1 Jun 2010; revised 16 Jul 2010; accepted 16 Jul 2010; published 27 Jul 2010

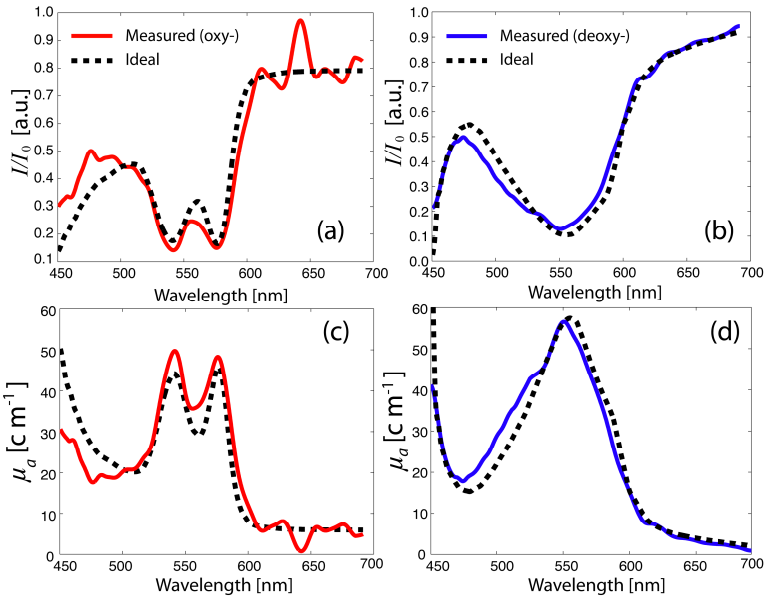

Fig. 3. Oxy-Hb (a) and deoxy-Hb (b) normalized absorption spectra, with Hb concentrations of 50 g/L and 68 g/L, respectively. The solid lines are experimentally measured, and the dotted black lines are the ideal. Oxy-Hb (c) and deoxy-Hb (d) measured and theoretical attenuation coefficients.

3.2 Hemoglobin concentrations

To calculate the Hb concentration (C_{Hb}), the absorption coefficient may be expressed in terms of the extinction coefficient, $\varepsilon(\lambda)$, which is independent of C_{Hb}: $\mu_a(\lambda) = C_{Hb} \cdot \varepsilon(\lambda)$. Here, all constants have been included in ε, where the Hb molecular weight used is *MW = 64500 g/mole*. Thus, by taking the natural log of Eq. (2), and substituting for $\mu_a(\lambda)$, we obtain,

$$-\ln\left(\frac{I(\lambda,L)}{I_0}\right) = C_{Hb} L\varepsilon(\lambda) - \ln(r). \qquad (3)$$

Note that $\varepsilon(\lambda)$ values for oxy-/deoxy- Hb are tabulated and are readily available (Fig. 1 [15],).

For each of the prepared samples, we analyze the absorption profiles of 25 distinct spatial locations, where the spectra are processed as described in section 3.1. Then, using Eq. (3), and known thickness L (which may be obtained from imaging), we calculate the concentration by fitting the data to a line of the form $\boldsymbol{y = mx + b}$, using a linear least squares method. Here, $\boldsymbol{x}$ is ether the oxy- or deoxy- Hb extinction coefficient and the computed $\boldsymbol{m} = C_{Hb}L$. This procedure was repeated for 6 different concentrations. The results are summarized in Fig. 4.

We find that the measured and expected concentration values are in excellent agreement, with $R^2_{oxy} = 0.9957$ and $R^2_{deoxy} = 0.9600$. The average standard deviation for all measurements is 3.10 g/L (no statistical significance was observed between the oxy- and deoxy- Hb values, *p-val = 0.82*). This value represents the lower limit of Hb concentration that may be detected at this depth. A more heuristic parameter, however, is obtained by multiplying the minimum measurable concentration by the depth, which gives a depth-independent value—this gives $C_{Hb\text{-}min}$ = 1.2 g/L at 1 mm (herein noted as g/L-mm). It is worth highlighting here that the total Hb concentration in normal tissue has been reported to be ~1.8 g/L, and as much as 3.2 times higher for cancerous tissue [3].

#129416 - $15.00 USD Received 1 Jun 2010; revised 16 Jul 2010; accepted 16 Jul 2010; published 27 Jul 2010

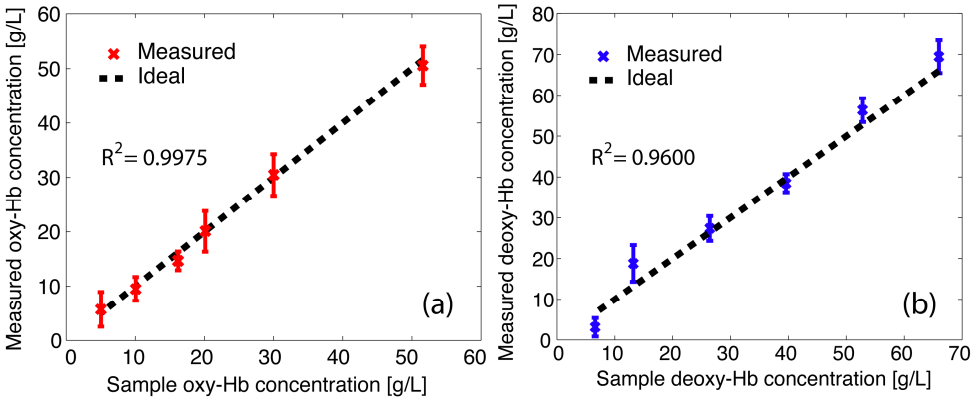

Fig. 4. Measured hemoglobin concentration for oxy- (a) and deoxy- (b) Hb samples. Error bars represent a standard deviation from the mean of 25 measurements.

3.3 Oxygen saturation

In biological samples, absorption will also depend on the oxygen saturation state of Hb. Thus, a more accurate model of the expected signal in biological samples is given by Eq. (4),

$$I(\lambda, L) = rI_0 \exp\left(-L\left[\varepsilon_{HbO_2}(\lambda)C_{HbO_2} + \varepsilon_{Hb}(\lambda)C_{Hb}\right]\right) \tag{4}$$

where ε_{HbO2}, ε_{Hb}, C_{HbO2} and C_{Hb} are the extinction coefficients and concentrations for oxy-/deoxy- Hb, respectively. This, in turn, can be written as an overdetermined set of linear equations to solve for C_{HbO2} and C_{Hb},

$$-\frac{1}{L}\ln\begin{bmatrix} \frac{I}{I_0}(\lambda_1) \\ \frac{I}{I_0}(\lambda_2) \\ \vdots \\ \frac{I}{I_0}(\lambda_n) \end{bmatrix} = \begin{bmatrix} \varepsilon_{HbO_2}(\lambda_1) & \varepsilon_{Hb}(\lambda_1) & -1/L \\ \varepsilon_{HbO_2}(\lambda_2) & \varepsilon_{Hb}(\lambda_2) & -1/L \\ \vdots & \vdots & \vdots \\ \varepsilon_{HbO_2}(\lambda_n) & \varepsilon_{Hb}(\lambda_n) & -1/L \end{bmatrix} \begin{bmatrix} C_{HbO_2} \\ C_{Hb} \\ \ln(r) \end{bmatrix} \tag{5}$$

where λ_i for $1 \le i \le n$ are the discretely measured wavelengths within the operating region. Finally, partial oxygen saturation (S_{O2}) can be calculated by Eq. (6),

$$S_{O_2} = \frac{C_{HbO_2}}{C_{HbO_2} + C_{Hb}}. \tag{6}$$

Based on this analysis, it is clear that the ability to correctly measured oxygen saturation depends on the extent to which the method, given by Eq. (5), can correlate the measured data to the correct chromophore species, i.e., oxy- or deoxy- Hb. For example, if $\boldsymbol{y}$ is the measured data and $\boldsymbol{x}$ is the model in question, the correlation of $\boldsymbol{y} = \boldsymbol{x}$, using a linear least squares fit, determines how well the model fits the data. For this example, a high correlation value signifies that the model describes the observations well; more importantly, for our study, high correlation values indicate that the method will clearly distinguish between the contributions to attenuation from the oxy- species and the deoxy- species. Therefore, a high correlation value suggests that oxygen saturation levels can be measured correctly.

To determine the lowest concentration at which oxygen saturation states may be correctly measured, the correlation coefficient of the linear regression used to determine concentration

#129416 - $15.00 USD Received 1 Jun 2010; revised 16 Jul 2010; accepted 16 Jul 2010; published 27 Jul 2010

in section 3.2 was calculated. To execute this analysis, a limited bandwidth ranging from 520 nm to 585 nm was used, which was chosen to highlight the disparity between ε_{HbO2} and ε_{Hb}. The correlation coefficient between the theoretical ε_{HbO2} and ε_{Hb} in this region, delineated by the dotted black lines in Fig. 1(b), is ~0. The results are summarized below, where Fig. 5(a) shows the correlations of the oxy-Hb data when compared to the oxy- and deoxy- Hb extinction coefficients, and Fig. 5(b) shows the results for the deoxy-Hb data.

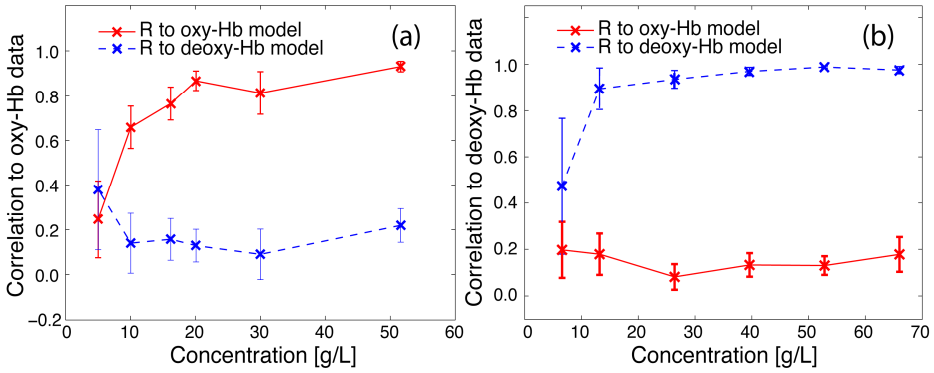

Fig. 5. (a) Correlation coefficients between the oxy-Hb data and the oxy-/deoxy- Hb extinction coefficients at varying concentrations. (b) Correlation coefficients between the deoxy-Hb data and the oxy-/deoxy- Hb extinction coefficients at varying concentrations.

Good agreement (R>0.65) is observed for concentration values higher than 10 g/L if the data are compared to the correct corresponding species (i.e., oxy-Hb data to oxy-Hb model, etc.); further, there exist a sharp cut off below this point. In contrast, a low correlation value (R<0.2) is observed for all concentrations above 10 g/L if the data are compared to the wrong model. This suggests that, while concentration values may be determined as low as 1.2 g/L-mm, oxygenation states can only be accurately determined for concentrations above 4 g/L-mm (= 10 g/L × 0.4 mm).

4. Discussion

In this paper, we have shown the ability to measure Hb concentrations as low as 1.2 g/L-mm, and over a wide range, with very good agreement with the expected values ($R^2 > 0.9$). As stated in section 3.2, normal (colorectal) tissue Hb concentrations have been reported to be ~1.8 g/L [3]: this indicates that normal Hb concentrations are well within the range of SOCT detection at depths greater than ~0.67 mm (= 1.2 g/L-mm / 1.8 g/L). Furthermore, abnormal (or cancerous) concentration values have been observed to be ~3.2 times greater than normal (~5.7 g/L) [3], hence these are also detectable using our methods.

We have also determined that oxygen saturation states may only be correctly measured at concentrations higher than 4 g/L-mm. These values fall outside the range of detection for normal tissue, where penetration depths would need to be greater than L = 2 mm. However, for cancerous tissue, the expected concentration values are within feasible detection range (L<1 mm). Further, the expected concentration of Hb within blood (150g/L) would allow oxygen saturation to also be detected with this method.

It is worthwhile to compare these results with previous works aimed at extracting absorption properties from Hb samples using SOCT: First, Faber et al. showed the feasibility of extracting Hb absorption coefficients [9] and later oxygenation saturation states [16] in blood, where concentrations are typically 150 g/L. Detection for those studies was centered about the isobestic point around 800 nm. Later, it was reported that, due to the contributions of scattering, absolute chromophore quantification was not feasible [17]. These conclusions result, in part, from the choice of wavelength range, which shows relatively weak Hb absorption around 800 nm. Additionally, methods have been presented that separate

#129416 - $15.00 USD Received 1 Jun 2010; revised 16 Jul 2010; accepted 16 Jul 2010; published 27 Jul 2010

absorption and scattering contributions [18,19] which may help lead to determination of absorber concentration within tissues.

Recently, Bosschaart *et al*. used a similar system as the one presented here (including spectral detection range), named low-coherence spectroscopy (LCS) to assess absorption [10]. Using scattering polystyrene spheres and a green dye for absorption, it was found that LCS was a promising technique for *in-vivo* determination of tissue absorption properties regardless of scattering. This further supports the claim that the approach used here can be applied to tissue, despite the fact that the samples did not contain scatterers. Like the work presented in [10], the technique presented here offers higher sensitivity by operating in the visible wavelength region. However, the methods for detecting absorption differ: In this study, the DW method is used, which enables high spectral resolution along with the same spatially resolved imaging capabilities as OCT. In [10], the method requires translation of both the sample and reference arms, and must also sacrifice spatial resolution to achieve the spectral resolution required for quantification.

In summary, we have shown that our pfdOCT system using the DW method is capable of measuring hemoglobin concentrations as low as those found in healthy and cancerous tissue. This further supports the hypothesis that SOCT may improve upon current optical techniques that are used to assess tissue properties for disease diagnosis. Future works will aim to implement this technique to assess Hb concentration within tissue.

Acknowledgments

We gratefully acknowledge Joseph Bonaventura for supplying his expertise on hemoglobin. This research has been supported by grants from the National Institutes of Health (NIH) (NCI 1 R01 CA138594-01).

#129416 - $15.00 USD Received 1 Jun 2010; revised 16 Jul 2010; accepted 16 Jul 2010; published 27 Jul 2010